P1.23 Structure and evolution of numerically simulated misocyclones along a snowband over the Shonai region on 25 January 2008

Wataru Mashiko[1)], Syugo Hayashi[1)], Kenichi Kusunoki[1)], Wataru Kato[2)], Yoshihiro Hono[2)], Toshiaki Imai[3)], Tetsuya Takemi[4)], Hanako Y. Inoue[1)], Kotaro Bessho[1)], Shunsuke Hoshino[1)], Masahisa Nakazato[1)], Hiroshi Yamauchi[1)], Keiji Adachi[2)], Keiji Araki[3)],Takaaki Fukuhara[3)],Toru Shibata[3)]
[1)] Meteorological Research Institute, Tsukuba, Japan
[2)] East Japan Railway Company, Saitama, Japan,
[3)] Researcher, Railway Technical Research Institute, Kokubunji, Tokyo, Japan,
[4)] Disaster Prevention Research Institute, Kyoto University, Kyoto, Japan

1. Introduction

On 25 January 2008, strong wind gusts (about 30 m s^{-1}) occurred locally in the Shonai region, coastal area of the Sea of Japan, during the passage of a developed snowband. Doppler radars detected a number of low-level misocyclones in the snowband, indicating that the near-surface wind gusts were associated with the misocyclones.

In order to clarify the structure and evolution of the misocyclones, we performed a high-resolution simulation with a horizontal grid spacing of 50 m.

2. Observed surface wind gusts

To study a mechanism and detection of wind gusts, a special observation has been carried out since 2007 winter around the Syonai region, which is located on the Japan Sea side in the northern Japan (Fig. 1). The major facilities for the observation include two Doppler radars and twenty-six automated surface weather instruments which are deployed in the Shonai plain at about 4-km intervals.

Strong surface wind gusts (28.8 m s^{-1} at Shonai airport and 31.3 m s^{-1} at C2 station, see Fig.1 for the geographical location) were observed at the coast in the Shonai region around 0530 JST (JST = UTC + 9 hours) on 25 January 2008 (Fig. 2). The wind gusts were accompanied with a slight pressure drop. In addition, the surface observtions indicates that the gusts occurred on the wind shear line (wind shift to the northward).

Corresponding author: Wataru Mashiko
Meteorological Research Institute, 1-1 Nagamine, Tsukuba, Ibaraki 305-0052, Japan
E-mail: wmashiko@mri-jma.go.jp

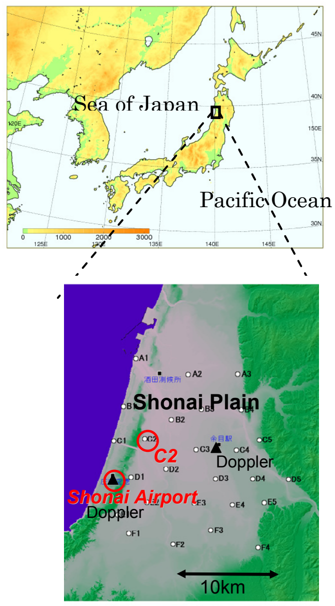

Fig. 1. Geographical locations around Shonai region.

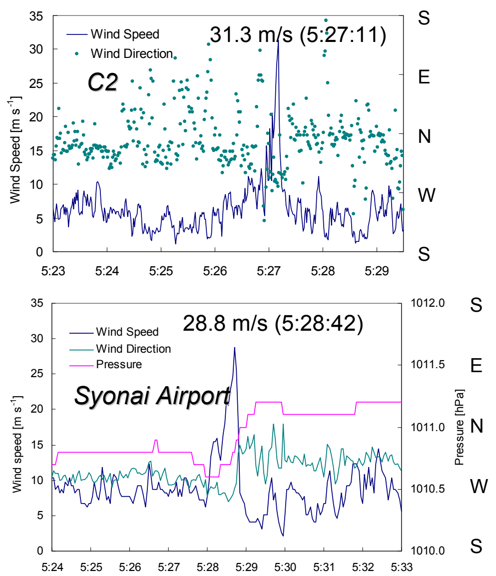

Fig. 2. Surface time series at (a) C2 station and (b) Shonai airport on 25 January 2008.

3. Overview of synoptic field

A moderate cold-air outbreak from the Eurasian landmass continued, and low pressure system passed on the northern side of Shonai region on 24 January (Fig. 3). Following the passage of the synoptic scale low, strong cold-air outbreak started from the rear side of the low with the northerly winds, which is represented by the NNW-SSE directed snowbands in the Radar images (Fig. 4). At the southern edge of them, the developed WNW-ESE-oriented snowband organized and moved southward. The snowband passed over the Shonai region around 0530 JST, which is temporally coincident with the observed gust occurrences.

Several low-level misocyclones were detected within this intense precipitation system by the Doppler radars (not shown).

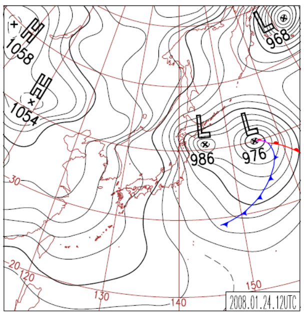

Fig. 3. Surface weather chart at 2100 JST on 24 January 2008.

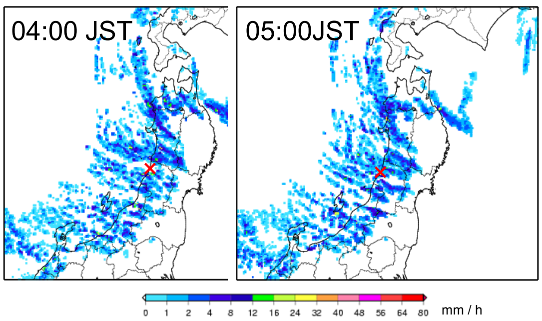

Fig. 4. Rainfall intensity estimated from Radar reflectivity at (a) 0400 JST and (b) 0500 JST on 25 January. Red "×" denotes the location of Shonai Plain.

4. Numerical model

The numerical model used in this study is the nonhydrostatic model (JMANHM; Saito et al. 2006) developed by the Japan Meteorological Agency (JMA). It is based on fully compressible equations with a map factor. The present study employed the bulk-type cloud microphysics scheme with six water species: water vapor, cloud water, rain, cloud ice, snow, and graupel (Lin et al. 1983; Murakami 1990). The turbulence closure scheme is based on Deardorff (1980) and predicts the turbulence kinetic energy.

Quadruply nested one-way grids are used to conduct high-resolution model integrations (Fig. 5). Hereafter, the experiments with horizontal grid spacings of 5 km, 1 km, 250 m, and 50 m are referred to as NHM5km, NHM1km, NHM250m, and NHM50m, respectively. The initial and boundary conditions of NHM5km are provided from an operational regional analysis of JMA that adopted a four-dimensional variational data assimilation system (JMA 2007). The present simulations include complex real topography and surface friction.

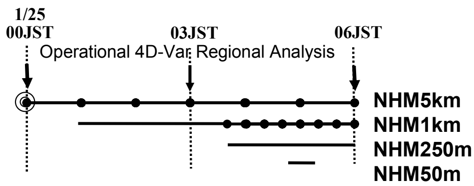

Fig. 5. Relationship of nesting.

5. Brief verification of simulation results

NHM1km successfully reproduced the intense precipitation system at the southern edge of the NNW-SSE directed snowbands caused by the passage of low pressure system (Fig. 6). However, it passed over the Shonai region about 30-min earlier than the observation.

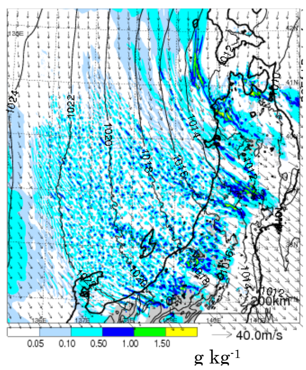

Fig. 6. Horizontal distribution of the mixing ratio of hydrometeors at a height of 1 km at 0500 JST simulated by NHM1km. Arrows indicate wind vectors, and contour lines denote sea level pressure at 2 hPa intervals.

Figures 7a and b show the simulation results around the Shonai region by NHM250m. A remarkable shear line was formed at low level between the north-northwesterly and northwesterly (Fig. 7a). Several extremes of vertical vorticity exist along it. The shear line is located at the southern side of the developed snowband (cf., Fig. 7a and 7b).

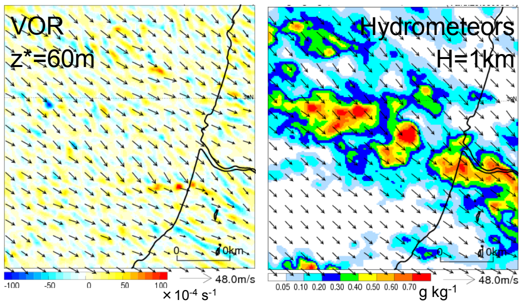

Fig. 7. Horizontal cross-section of (a) vertical vorticity at a height of 60 m and (b) hydrometeors at a height of 1 km at 0500 JST simulated by NHM250m. Arrows indicate wind vectors.

6. Wave-like structure along a low-level shear line simulated by NHM50m

The evolution of vertical vorticity around the low-level shear line is shown in Fig. 8. Wavelike disturbances (4~7 km wavelength) developed along the shear line in the snowband around the Shonai region.

Figure 9 shows the mean vertical cross sections of shear-line oriented horizontal wind across the shear line at 05:03:30 JST (hh:mm:ss JST). The horizontal wind shear is largest at lower levels. The width across the shear line is about 1km.

Figure 10 depicts the eddy-component from the averaged wind field along the shear line. We use another Cartesian coordinate system (x, y, z), with the x axis parallel to the shear line and the y axis normal to the shear line. It is found that the wave-like disturbances are prominent around the shear line. The kinetic energy conversions from the mean horizontal shear along the shear line can be written as,

$$-\overline{u'v'}\frac{\partial \overline{u}}{\partial y} \quad (1).$$

The distribution of eddy-component horizontal winds in Fig 10 indicates that the value of (1) is positive around the shear line, which implies that the kinematic energy is converted from the mean flow to the eddies. As the wavelike pattern was amplified, several vortical disturbances became prominent along the low-level shear line and exhibited characteristics of a misocyclone (M1 and M2 in Fig 8). They moved southeastward and subsequently landed on the Shonai region.

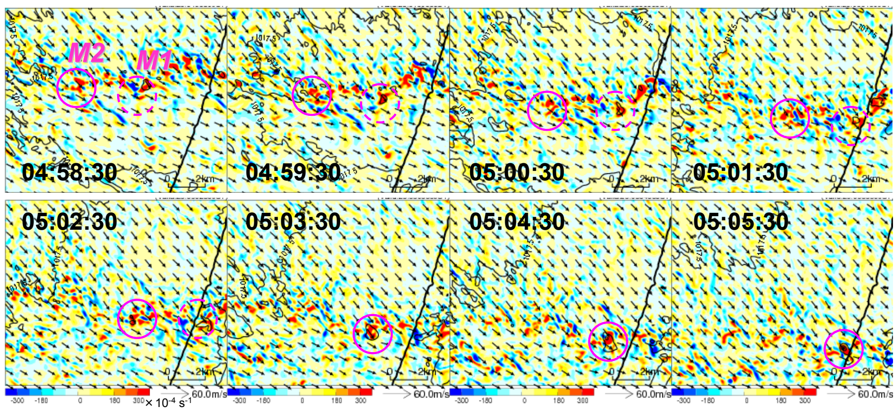

Fig. 8. Evolution of vertical vorticity at a height of 250m. Arrows indicate wind vectors.

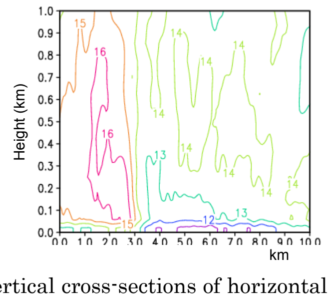

Fig. 9. Vertical cross-sections of horizontal wind velocity parallel to the shear line across it at 05:03:30 JST. Wind velocity is averaged along the shear line in 10 km

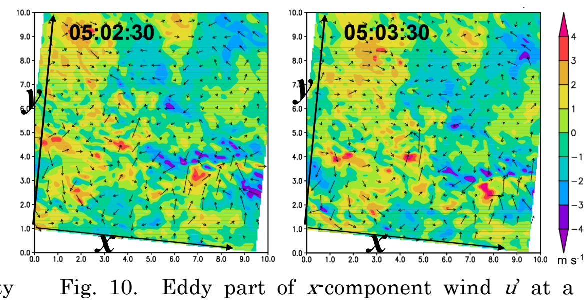

Fig. 10. Eddy part of x-component wind u' at a height of 250 m is shaded. Arrows indicate the eddy component horizontal wind (u', v').

7. Structure and evolution of a misocyclone (M2) simulated by NHM50m

One misocyclone (M2) had a strong cyclonic circulation of about 600 m diameter (peak-to-peak in wind velocity field) at a height of 500 m (Fig. 11a). Strong winds blows only on the right side of the M2's track, with exceeding 25 m s^{-1} including near the surface (Fig. 11c). The near-surface pressure deficit is about 1.5 hPa. Another noteworthy feature is that downdraft occupies near the center of the misocyclone (Fig.11b).

The misocyclone tilts toward downshear side. It exhibits a bottom-intensified and bottom-shrunken structure, and the near-surface vertical vorticity reaches 0.2 s^{-1} (Fig. 11d).

The vortical disturbance was generated below 300 m height and developed into the subsequent misocyclone structure (Fig.12), which is quite different from the evolution of a supercell-tornado.

8. Summary

In order to clarify the structure and evolution of misocyclones causing surface wind gusts over the Syonai region on 25 January 2008, numerical simulations were performed using quadruply nested grids with horizontal spacings of 5 km, 1 km, 250 m and 50 m. The simulation well reproduced the developed snowband accompanied by the low-level wind shear. Wavelike disturbances (4~7 km wavelength) developed along a shear line at low levels. The kinematic energy was converted from the mean flow of horizontal shear to the eddies. As the wavelike pattern was amplified, several vortical disturbances became prominent and developed into misocyclones. One misocyclone exhibited a bottom-intensified and bottom-shrunken structure, and the near-surface vertical vorticity reached 0.2 s^{-1}. Surface wind gusts exceeding 25 m s^{-1} existed only on the right side of misocyclone's track.

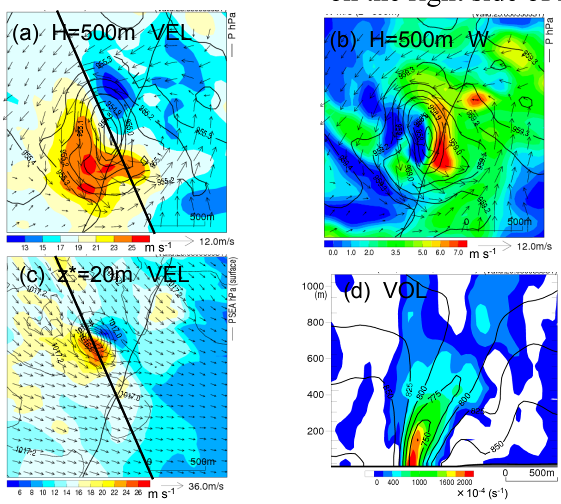

Fig. 11. Structure of a misocyclone (M2) at 05:03:30 JST. Horizontal cross-section of (a) horizontal velocity and (b) vertical velocity at a height of 500 m. Arrows denote storm-relative wind vectors. Pressure contour lines are drawn at 0.1 hPa intervals. (c) Horizontal wind velocity at a height of 20 m. Arrows denote ground-relative wind vectors, and contour lines indicate sea level pressure at 0.2 hPa intervals. (d) Vertical cross-section of vertical vorticity along a line shown in (a) and (c). Contour lines indicate pressure perturbation at 25 Pa intervals.

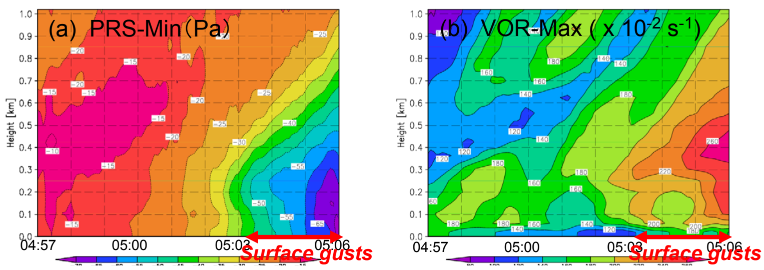

Fig. 12. Time-height cross-section of (a) minimum pressure perturbation and (b) maximum vertical vorticity averaged horizontally over 500 m square for the misocyclone (M2) from 0457 to 0506 JST. Each value was calculated with a 1.25 km radius of M2 center at a height of 250 m.

Acknowledgments.

This research is supported by the Program for Promoting Fundamental Transport Technology Research from the Japan Railway Construction, Transport and Technology Agency (JRTT).

REFERENCES

Deardorff, J. W., 1980: Stratocumulus-capped mixed layers derived from a three-dimensional model. Bound.-Layer Meteor., 18, 495-527.

Japan Meteorological Agency, 2007: Outline of the operational numerical weather prediction at the Japan Meteorological Agency. pp 29-35. [Available from JMA, 1-3-4 Otemachi, Chiyoda-ku, Tokyo 100-8122, Japan.]

Lin, Y. H., R. D. Farley, and H. D. Orville, 1983: Bulk parameterization of the snow field in a cloud model. J. Climate. Appl. Meteor., 22, 1065-1092.

Murakami, M., 1990: Numerical modeling of dynamical and microphysical evolution of an isolated convective cloud –The 19 July 1981 CCOPE cloud. J. Meteor. Soc. Japan, 68, 107-128.

Saito, K., T. Fujita, Y. Yamada, J. Ishida, Y. Kumagai, K. Aranami, S. Ohmori, R. Nagasawa, S. Kumagai, C. Muroi, T. Kato, H.Eito, and Y. Yamazaki, 2006: The operational JMA nonhydrostatic mesoscale model. Mon. Wea. Rev., 134, 1266-1298.